Article

Efficient Process Development of Abiraterone Acetate by Employing Design of Experiments

Shravan Kumar Komati, Mukesh Kumar Madhra, Amarendhar Manda,
Sasikala Cheemalapati Venkata Annapurna, Gopal Chandru Senadi, Arthanareeswari Maruthapillai,*
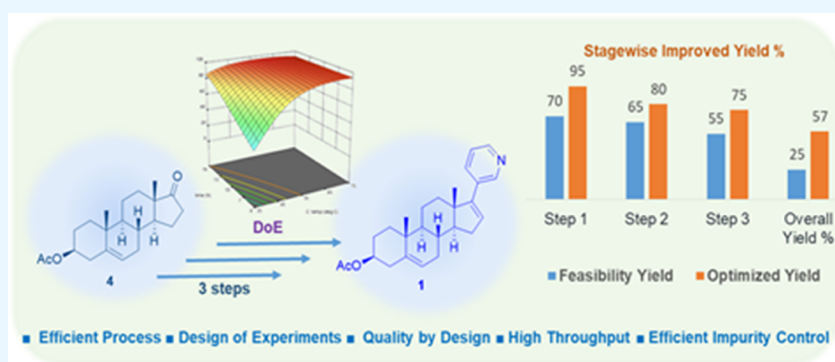and Rakeshwar Bandichhor*

ACCESS | Metrics & More | Article Recommendations | SI Supporting Information

ABSTRACT: This article describes an efficient process for the synthesis of abiraterone acetate by employing Quality by Design (QbD) principles and statistical design of experiments (DoE). It focuses on the identification of critical quality attributes (CQAs), the relationship between CQAs and material attributes (MAs), and critical process parameters (CPPs) for the synthesis of hydrazone, vinyl iodide intermediates, and final product. Risk assessment is employed to identify the probable critical factors involved in each chemical transformation. The design of experiments approach aided in controlling the formation of critical impurities in all three reactions, namely, deacylated impurity in the hydrazone intermediate, 17-methyl impurity in the vinyl iodide intermediate, and hydroxy and diene impurities in the final API. The process was developed such that we achieved 95, 85, and 82% selectivity and 99, 96, and 99% purity in hydrazone, vinyl iodide intermediate, and final API, respectively. This reflects improved throughput from 25 to 57% as a result of the subtle interplay of critical process parameters identified by DoE studies.

INTRODUCTION

Abiraterone acetate (Figure 1) is used to treat prostate cancer,[1] specifically corticosteroid for metastatic castration-resistant
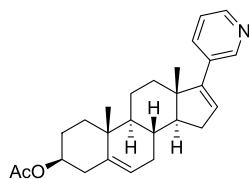

Figure 1. Chemical structure of abiraterone acetate **1**.

prostate cancer and metastatic high-risk castration-sensitive prostate cancer. Abiraterone is an active metabolite of abiraterone acetate in vivo, an androgen biosynthesis inhibitor that inhibits 17α-hydroxylase/C17,20-lyase (CYP17). This enzyme is expressed in testicular, adrenal, and prostatic tumor tissues and is essential for androgen biosynthesis. Interestingly, CYP17 catalyzes two sequential reactions, the first one being

pregnenolone and thereafter progesterone to their 17α-hydroxy derivatives by 17α-hydroxylase activity and subsequent formation of dehydroepiandrosterone (DHEA) and androstenedione, respectively, as a function of C17,20-lyase activity. Inhibition of CYP17 by abiraterone is found to increase adrenal mineralocorticoid production. It is also found that it decreases androgen production in the testes but does not affect androgen production by the adrenals.
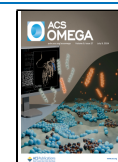
The manufacturing process of abiraterone acetate **1** involves three steps,[2,9] as shown in Scheme 1. The first step is the reduction of dehydroepiandrosterone-3-acetate **4** to hydrazone intermediate **3** through a partial Wolff−Kishner reduction

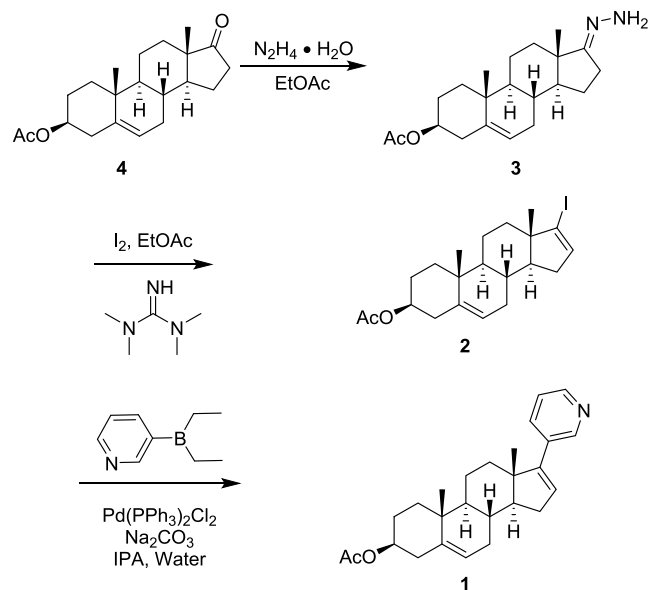**Scheme 1. Synthesis of Abiraterone Acetate 1**

method using hydrazine hydrate. Thereafter, the resultant is converted to vinyl iodide intermediate **2** through Barton vinyl iodide synthesis,[6] using iodine in the presence of tetramethyl-guanidine (TMG) base. Further, Suzuki–Mayura coupling is performed with BET (diethyl(3-pyridyl)borane) **7** in the presence of the Pd(PPh₃)₂Cl₂ catalyst and sodium carbonate base to give abiraterone acetate **1**.

■ RESULTS AND DISCUSSION

Hydrazone Intermediate 3 Synthesis. The synthesis of hydrazone intermediate 3 (Scheme 2) involves the addition of hydrazine hydrate to the stirred solution of dehydroepian-drosterone-3-acetate (DHEA acetate) **4** in ethyl acetate at ambient temperature, followed by refluxing for 10 h, affording 80% conversion and 70% isolated yield. In this transformation, incomplete reaction conversion along with the formation of deacylated impurity **5** (Figure 2) was observed to be about 5%.
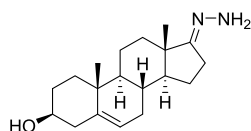

Figure 2. Chemical structure of deacylated impurity **5**.

This undesired substance impacts the process throughput and cost; foremost, it increases the load on the downstream process to meet the CQAs of hydrazone intermediate **3** (Scheme 2).

The synthetic process was evaluated using cause and effect analysis, listing possible causes to improve the selectivity,[12] which included process parameters like reaction temperature

Scheme 2. Synthesis of Hydrazone Intermediate 3
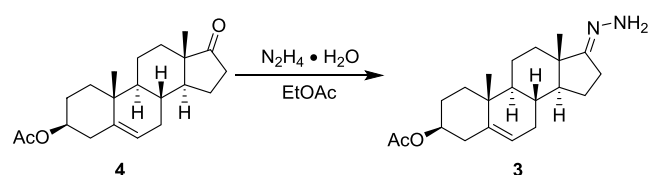
and time and material attributes like ethyl acetate quantity and hydrazine hydrate mole equiv, as depicted in Figure 3. Identified variables and their levels are described in Table 1. Based on this evaluation, a statistical multivariate experimentation approach was adopted to understand the reaction profile. Reaction mass samples were analyzed using the high-performance liquid chromatography (HPLC) technique by the area normalization method. A full factorial design was chosen for the experimenta-tion with four factors at two levels, leading to 16 experiments (2^4 = 16). To check the repeatability, four center points were added.

Statistical evaluation of the full factorial experimental data indicated that curvature was significant for all three responses, meaning that nonlinear behavior was present in the response variables. Further, augmentation with a central composite design was carried out to understand the nonlinear behavior, with an additional eight runs and two center points.[14,15] Table 2 depicts all experimental results. Analysis of variance (ANOVA) and multiple regression analyses were performed for all three responses individually. Higher temperatures for longer main-tenance time led to the maximum product **3** formation and minimum unreacted starting material **4**, and these two factors interacted with each other, as represented in Figures 4 and 5. Other factors like hydrazine hydrate equiv and ethyl acetate vol have no significant effect on product **3** formation. Ethyl acetate volume and hydrazine hydrate equiv are significant factors for the formation of deacylated impurity **5**. Higher ethyl acetate vol with lower hydrazine hydrate equiv will control the formation of deacylated impurity **5**, as represented in Figure 6. It is also observed that interaction of both material attributes exists on deacylated impurity **5** (detailed statistical analysis is given in the Supporting Information).

The summary from statistical analysis is that a temperature of more than 60 °C and a reaction time of 10 h are preferred parameters to maximize the hydrazone intermediate **3** and minimize DHEA acetate **4**. Above 14 vol of ethyl acetate and less than 5 mol equiv of hydrazine hydrate are preferable to control the formation of deacylated impurity **5**. Based on the downstream process capability, design space is created, as shown in Figure 7, by considering the following criteria: DHEA acetate **4** is not more than 1%, hydrazone intermediate **3** is not less than 95%, and deacylated impurity **5** is not more than 0.5%. The proven acceptable ranges (PARs) for the parameters are 14–15 vol of ethyl acetate, 1.3–5.0 equiv of hydrazine hydrate, and 60–70 °C reaction temperature with a maintenance time range of 10–16 h. Model efficiency was established by performing conformation experiments.

Vinyl Iodide Intermediate 2 Synthesis. Vinyl iodide intermediate **2** is prepared by following the Barton vinyl iodide synthesis[3−6] process, and hydrazone intermediate **3** is oxidized to corresponding vinyl iodine intermediate **2** using iodine in the presence of TMG[7] (Scheme 3). The synthesis process involves slow addition of hydrazone intermediate **3** in ethyl acetate to a mixture of iodine and TMG at 15–20 °C, followed by maintaining for 2–3 h at the same temperature. HPLC analysis of the reaction mass shows only 30% required product **2**. Two related substances were mainly observed, around 20% of each. One was *gem*-diiodide, which would convert into desired product **2** upon heating to 70–80 °C, as mentioned in Barton vinyl iodide synthesis,[7] and the other related substance was 17-methyl impurity **6** (Figure 8). Apart from these two impurities, DHEA acetate **4** was also observed at around 5%. Due to these impurities, the maximum isolated yield obtained was about 65%. Optimization of reaction conditions tended to improve the
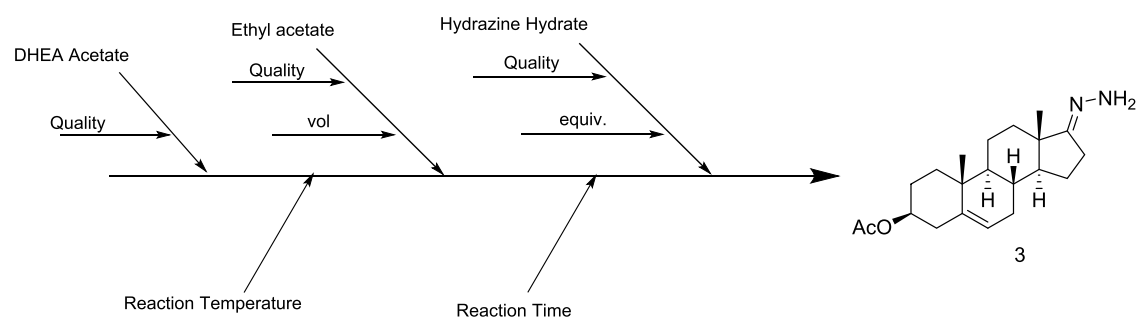
Figure 3. Cause and effect analysis for hydrazone intermediate **3** synthesis.

Table 1. Factors Studied for Hydrazone Intermediate 3 Synthesis

s. no.	variables	unit	low	high
1	hydrazine Hydrate	equiv	1.3	6.0
2	ethyl acetate	vol	4	15
3	temperature	°C	35	75
4	time	h	4	16

conversion and selectivity using the design of experiments (DoE)[16−17,18,19,20] approach. In the DoE study, based on the risk assessment using fishbone analysis (Figure 9), three critical parameters, mole equivalents of iodine, TMG, and reaction temperature, were identified. Table 3 depicts factors and their levels.

A full factorial design was selected. Table 4 depicts the HPLC data of the experimental design.

Experimental data reveal more than 99% of reaction conversion in all of the experiments. As per the statistical analysis of vinyl iodide intermediate **2**, TMG mole equiv has a positive effect, which means byproduct formation will increase by increasing the TMG mole equiv. Iodine mole equiv interacts with reaction temperature, as depicted in Figure 10. Similarly, 17-methyl impurity **6** is negatively influenced by iodine mole equiv and positively influenced by TMG mole equiv. Surprisingly, reaction temperature does not have any significant effect on the formation of **6**. This indicates that a lower mole

Table 2. Experimental Data of Hydrazone Intermediate 3

run	space type	ethyl acetate (vol)	hydrazine hydrate (equiv)	temp (°C)	time (h)	hydrazone intermediate 3 (%)	DHEA acetate 4 (%)	deacylated impurity 5 (%)
1	factorial	4.0	1.30	35	16	84.93	17.20	0.95
2	factorial	4.0	6.00	75	4	91.72	0.30	6.07
3	center	9.5	3.65	55	10	94.03	3.98	0.91
4	factorial	4.0	1.30	75	16	86.76	0.80	0.58
5	factorial	15.0	1.30	75	16	94.93	3.00	0.35
6	factorial	15.0	6.00	35	16	80.44	27.10	0.61
7	factorial	15.0	1.30	35	4	68.03	44.8	0.33
8	center	9.5	3.65	55	10	94.23	3.40	0.91
9	factorial	4.0	6.00	35	16	85.08	14.0	4.20
10	center	9.5	3.65	55	10	93.41	4.58	0.94
11	factorial	15.0	6.00	75	16	97.66	0.00	1.02
12	factorial	15.0	6.00	75	4	96.92	2.40	1.01
13	factorial	15.0	1.30	35	16	87.97	19.10	0.30
14	factorial	4.0	6.00	35	4	34.72	69.80	2.21
15	factorial	15.0	6.00	35	4	10.14	90.90	0.00
16	center	9.5	3.65	55	10	94.79	3.53	0.99
17	factorial	4.0	6.00	75	16	86.01	0.10	6.90
18	factorial	4.0	1.30	35	4	14.35	85.60	0.23
19	factorial	15.0	1.30	75	4	90.64	13.01	0.48
20	factorial	4.0	1.30	75	4	94.71	2.60	1.08
21	axial	9.5	1.30	55	10	91.30	12.80	0.27
22	axial	15.0	3.65	55	10	95.95	3.60	0.62
23	center	9.5	3.65	55	10	94.98	4.90	0.71
24	center	9.5	3.65	55	10	94.90	4.80	0.70
25	axial	9.5	3.65	55	16	96.51	1.30	0.76
26	axial	4.0	3.65	55	10	93.45	1.80	2.36
27	axial	9.5	6.00	55	10	95.56	2.30	1.65
28	axial	9.5	3.65	35	10	70.88	45.40	0.45
29	axial	9.5	3.65	55	4	81.60	28.10	0.56
30	axial	9.5	3.65	75	10	97.27	0.04	0.96

a. Main Effects Graph
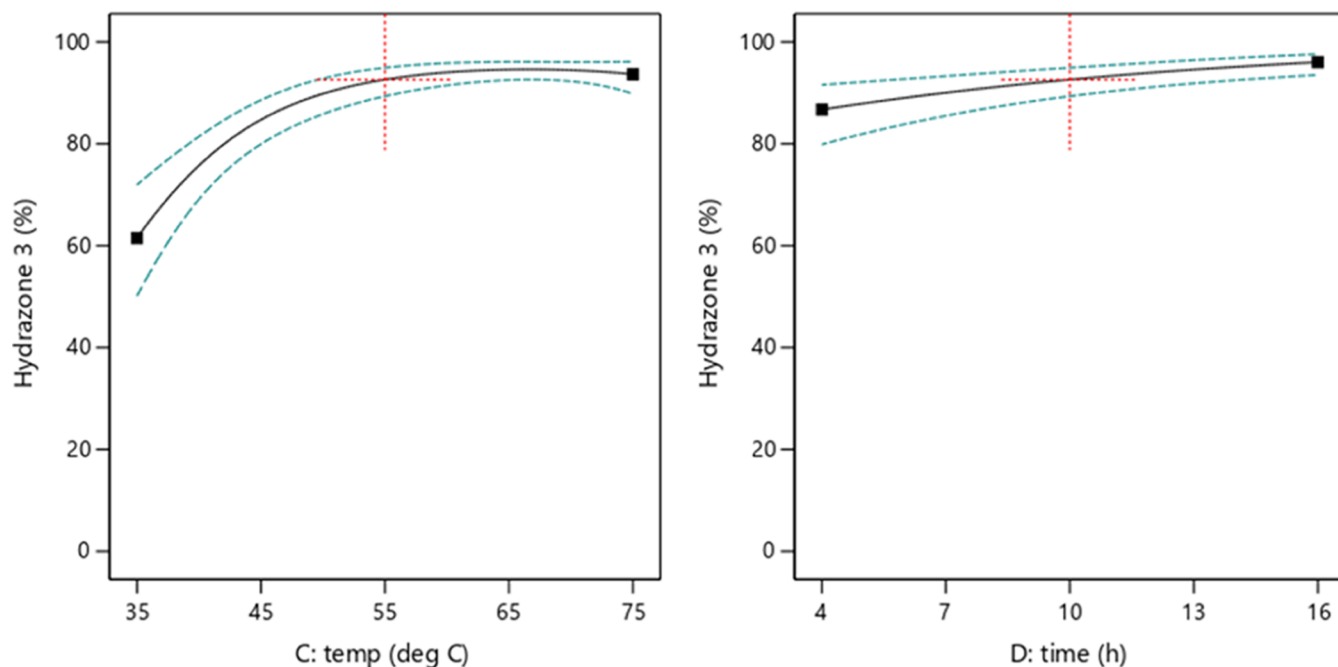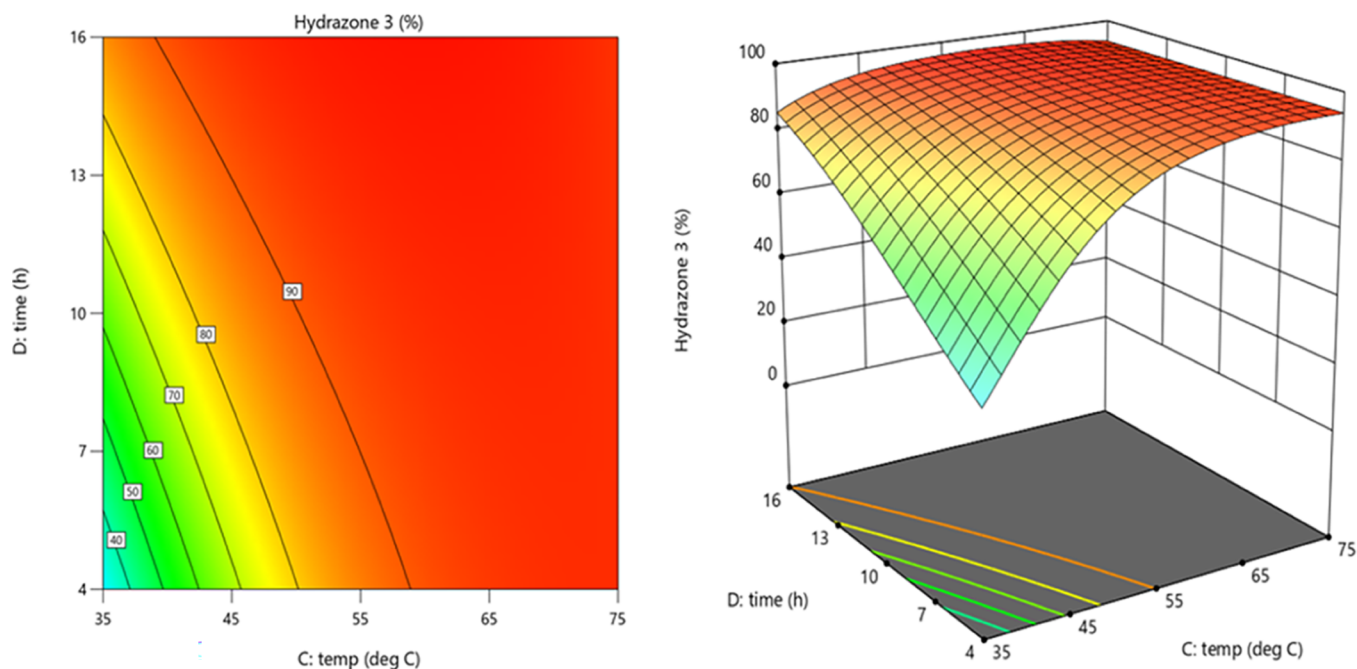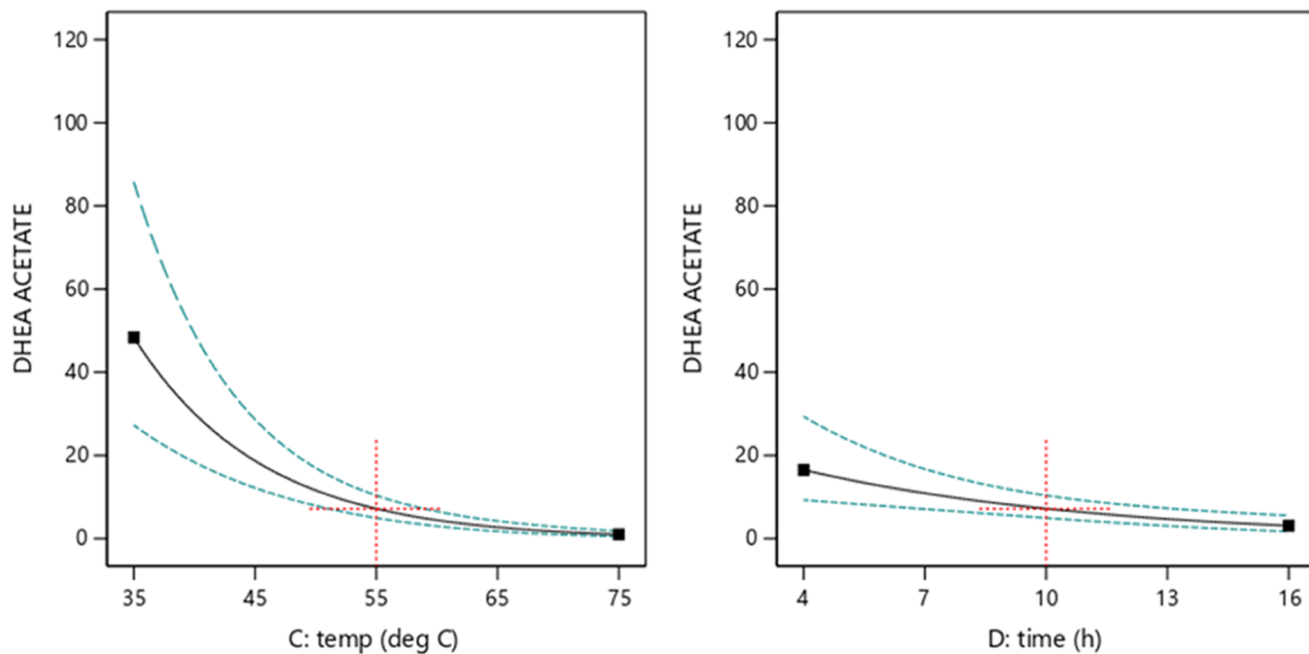

b. Contour Graph and 3D Graph

Figure 4. Graphical representation of hydrazone intermediate **3**.

ratio of iodine and a higher mole ratio of TMG control the formation of **6**, as portrayed in Figure 11. DHEA acetate is negatively influenced by the iodine mole equiv and TMG mole equiv, resulting in the formation of DHEA acetate **4**, which was found to be reduced by increasing the iodine and TMG mole ratio, as depicted in Figure 12. Factor settings were optimized to maximize the desirability for the criteria of vinyl iodide intermediate **2** is not less than 85%, DHEA Acetate **4** is not more than 2%, and 17-methyl impurity **6** is not more than 9%.

a. Main Effects Graph

b. Contour Graph and 3D Graph
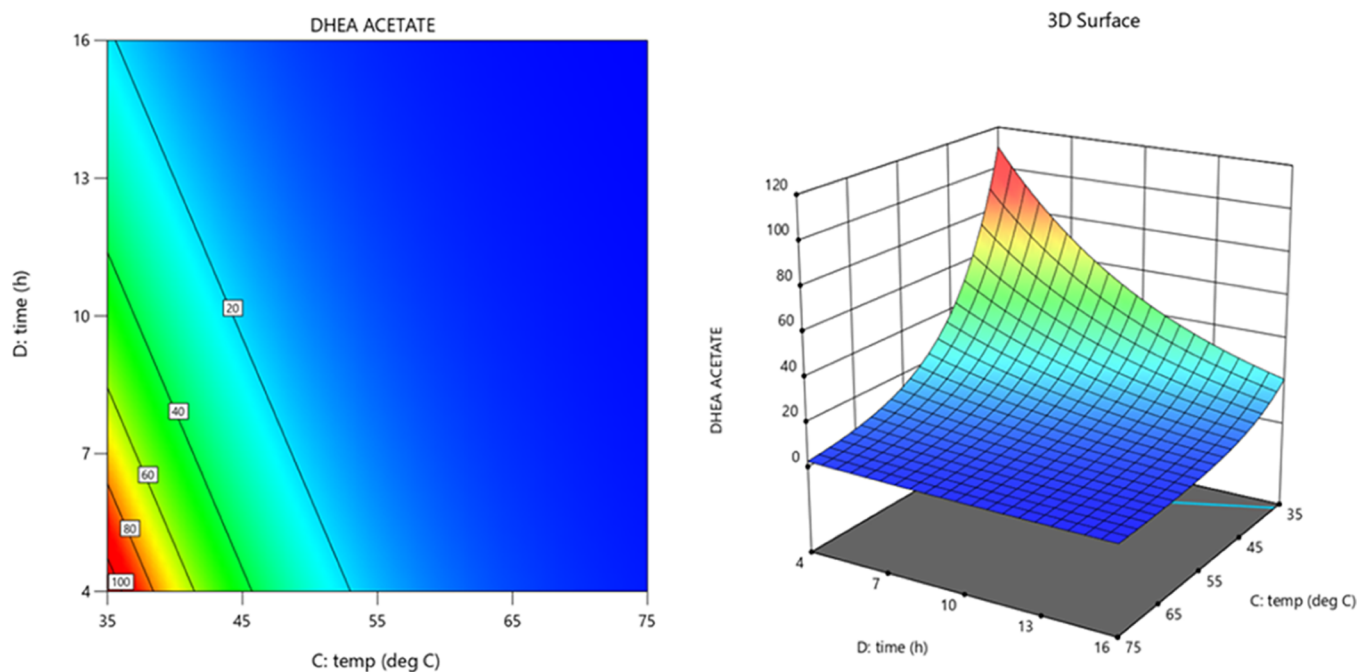
Figure 5. Graphical representation of DHEA acetate **4**.

Design space was established and validated, as shown in Figure 13.

Suzuki Coupling: Abiraterone Acetate 1 Synthesis. Abiraterone acetate **1** was prepared by reacting vinyl iodide intermediate **2** with BET **7** in the presence of Na_2CO_3 base and the bis(triphenylphosphine)palladium(II)dichloride catalyst in aqueous IPA as a solvent at elevated temperature (Scheme 4). In this process, two critical impurities were observed in reaction mass parallel to the product: the acetyl functional group hydrolyzed to get hydroxy impurity **8** (Figure 14) and the acetyl functional group eliminated to form 3,4 double-bonded diene[8] **9** (Figure 15) at about 5 and 2%, respectively. These two impurities were critical to meet the desired quality of drug substance **1**. Fishbone analysis (Figure 16) was performed and

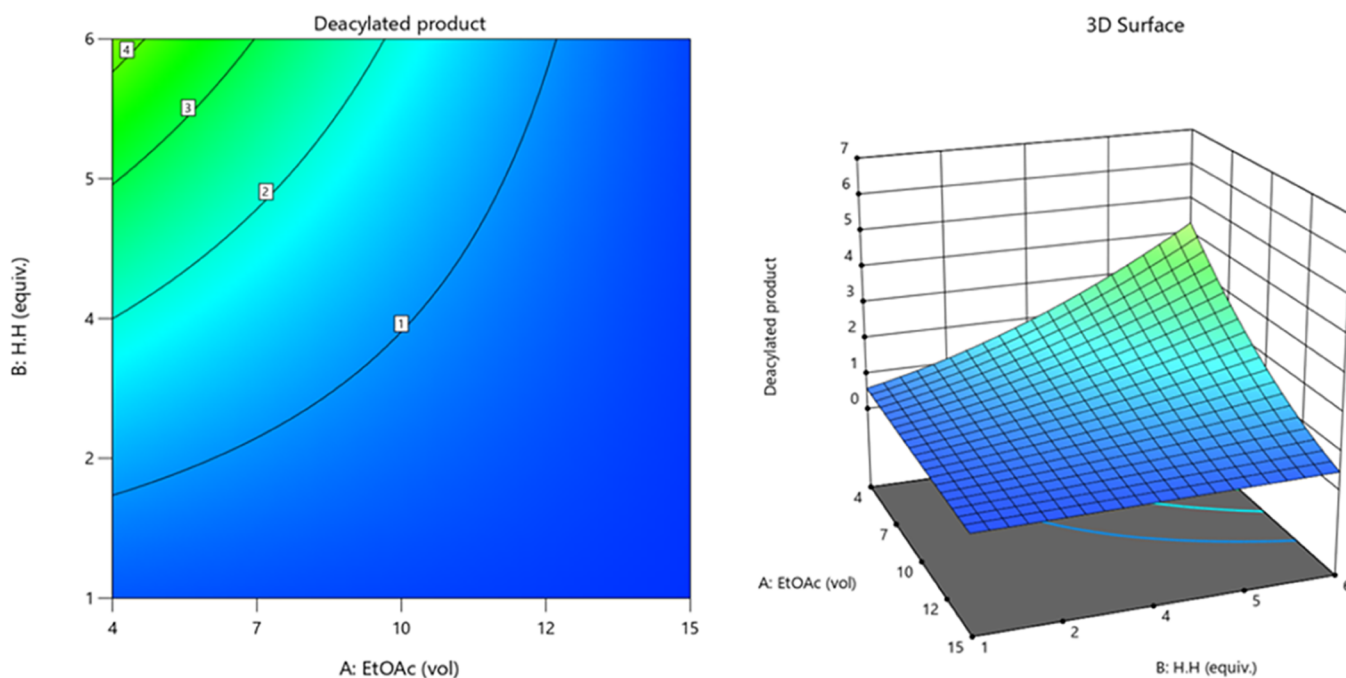## **a**. Main Effects Graph
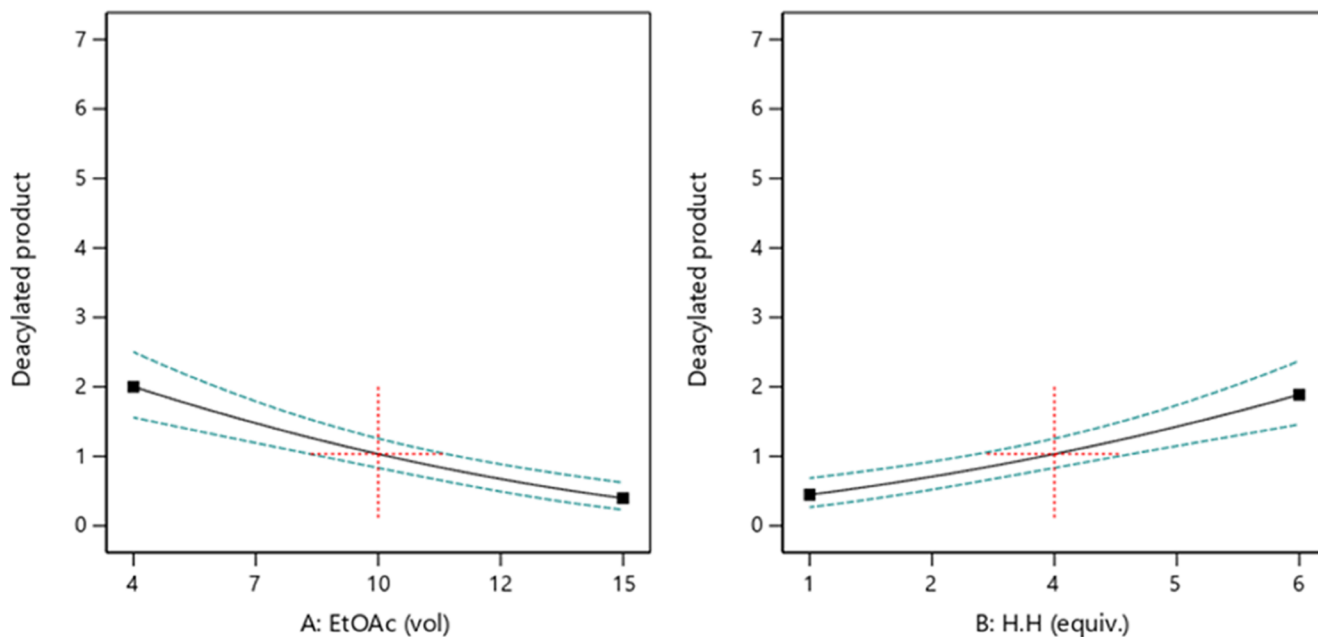
b. Contour Graph

Figure 6. Graphical representation of deacylated impurity **5**.

identified IPA vol, BET **7** equiv, and sodium carbonate equiv as critical factors for the formation of impurities, as captured in Table 5. Based on the preliminary experimental data, water vol, reaction temperature, and catalyst loading were kept constant. A full factorial design was selected to estimate the main effects and two factors' interactions by conducting 10 trials, including two center points. Reaction mass samples were monitored by HPLC, as presented in Table 6.

Statistical evaluation of experimental data revealed that vinyl iodide intermediate **2** was observed to be less than 0.5% in all experiments. Formation of product **1** was influenced by BET **7** equiv, which had a negative effect. It also had interactions with IPA vol and Na_2CO_3 equiv, and all three factors also interacted
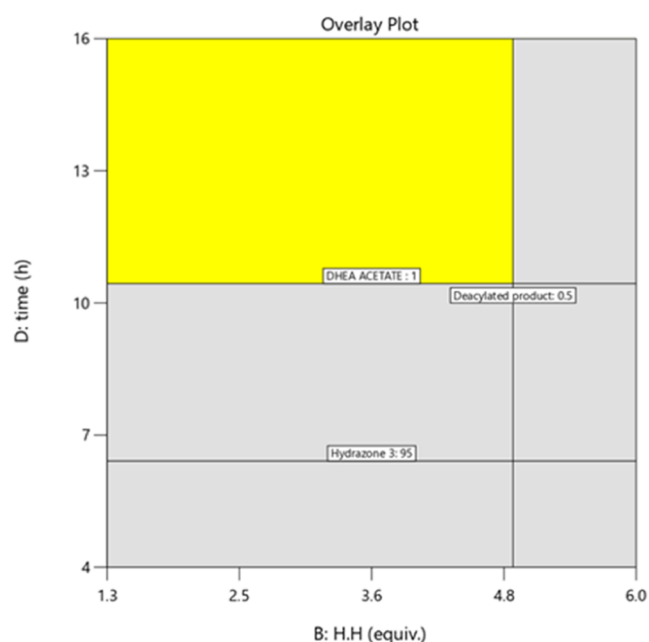
Figure 7. Design space for hydrazone intermediate **3** (14 vol of EtOAc and 70 °C temperature).

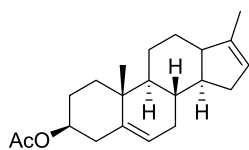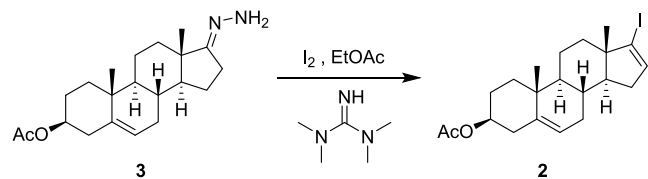**Scheme 3. Synthetic Scheme of Vinyl Iodide Intermediate 2**

Figure 8. Chemical structure of 17-methyl impurity **6**.

with each other, as depicted in the Pareto chart. Lower BET **7** equiv and higher Na_2CO_3 equiv are preferable to enhance the formation of product **1**, as represented in Figure 17.

For hydroxy impurity **8**, BET and Na_2CO_3 equiv values have a positive effect, and lower mole ratios are preferable to minimize

Table 3. Factors Studied for Vinyl Iodide Intermediate 2 Synthesis

s. no.	variables	units	low	high
1	iodine	equiv	2.0	3.0
2	TMG	equiv	5.0	10.0
3	reaction temp	°C	0	30

Table 4. Experimental Data of Vinyl Iodide Intermediate 2

run	iodine equiv	TMG equiv	reaction temp °C	vinyl iodide **2** %	17-methyl impurity **6** %	DHEA acetate **4** %
1	3.0	5.0	0	81.45	12.79	3.70
2	2.0	10.0	0	86.35	7.29	2.42
3	3.0	5.0	30	83.12	13.75	2.97
4	2.0	5.0	0	84.27	11.30	4.15
5	2.0	10.0	30	85.27	7.47	2.43
6	2.5	7.5	15	86.12	10.56	2.78
7	2.0	5.0	30	85.10	10.85	3.57
8	2.5	7.5	15	85.41	9.74	2.42
9	3.0	10.0	0	83.10	9.78	1.31
10	3.0	10.0	30	84.21	9.28	0.65

the formation of **8**. IPA vol has interactions with BET and Na_2CO_3 equiv. Contour graphs represent higher IPA vol, and lower Na_2CO_3 equiv values are preferable to minimize the formation of **8**, as shown in Figure 18.

Similarly, diene impurity **9** was influenced by all three factors and the interaction between IPA vol and BET equiv, as shown in Figure 19. IPA vol has a negative effect on this impurity; increasing the IPA vol minimizes the formation of diene impurity **9**. However, BET **7** and Na_2CO_3 equiv values have a positive effect; increasing the mole ratio of these two materials will increase diene impurity **9** formation. Lower BET equiv, higher IPA vol, and lower Na_2CO_3 equiv. are desired to minimize the diene impurity **9** formation, as represented in Figure 17. Design space was established and verified for the criteria of product **1** not less than 82%. It is also found that hydroxy impurity **8** is not more than 1%, and diene impurity **9** is not more than 0.8%, as shown in Figure 20. Derived operating ranges were 0.95−1.05 equiv of BET **7**, 4−5 equiv of Na_2CO_3, and 5−6 vol of IPA.

Green Chemistry Comparatives. Eventually, we compared the greenness of the processes of feasibility to the optimized procedure disclosed in this report. It transpired that the optimized process indicated lower PMI values, which were
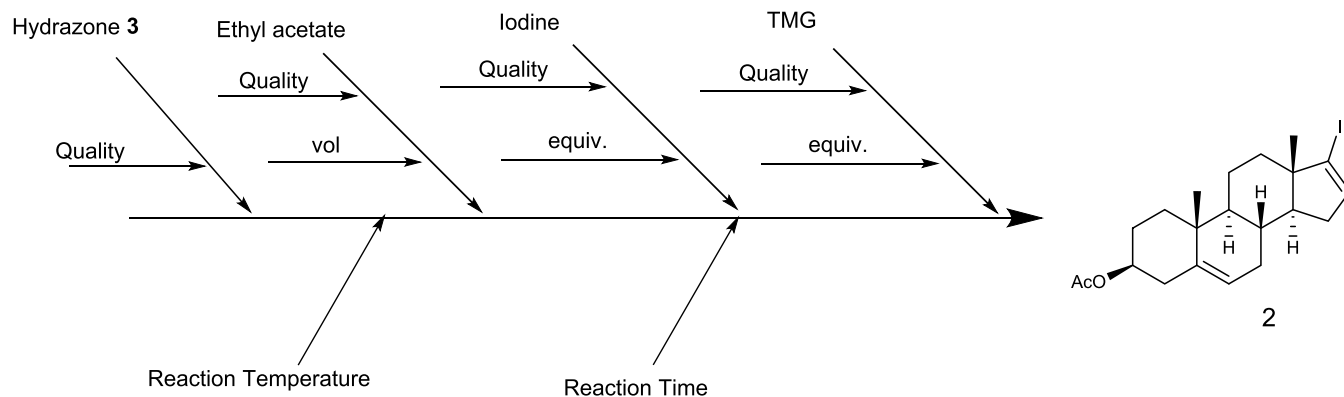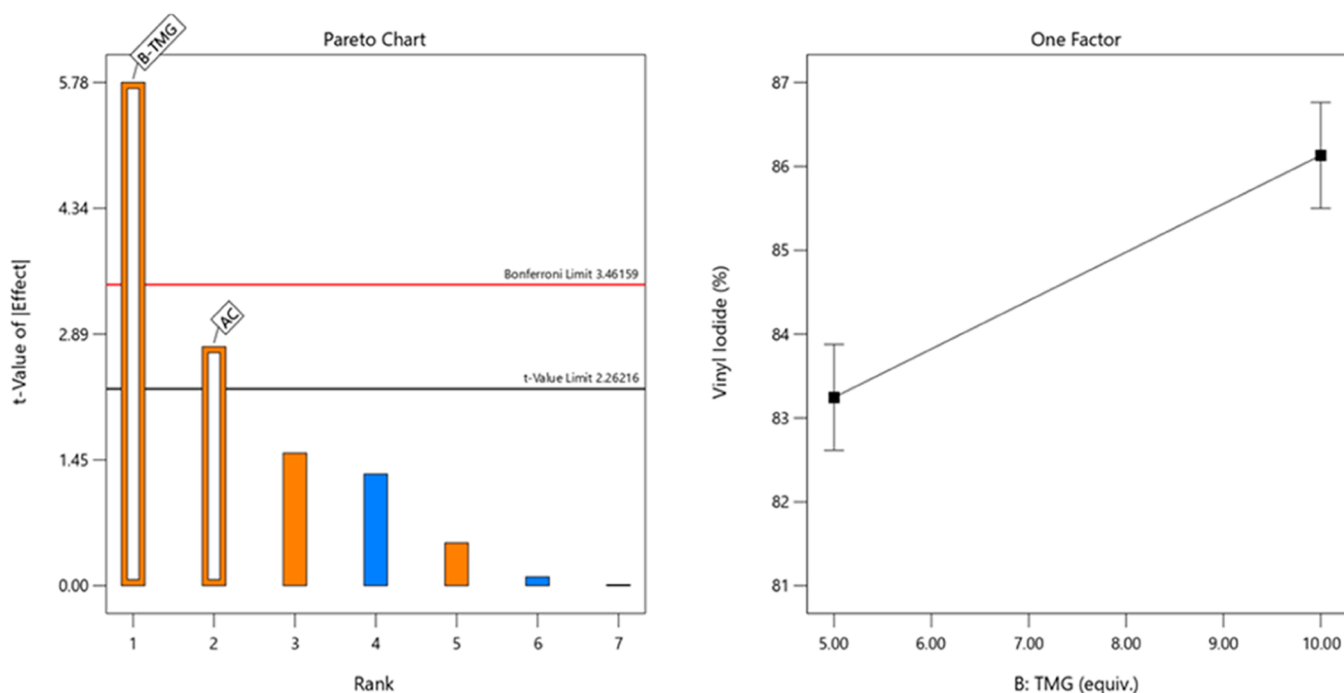

Figure 9. Cause and effect analysis for vinyl iodide intermediate **2** synthesis.

a. Pareto Chart and Main Effect Plot

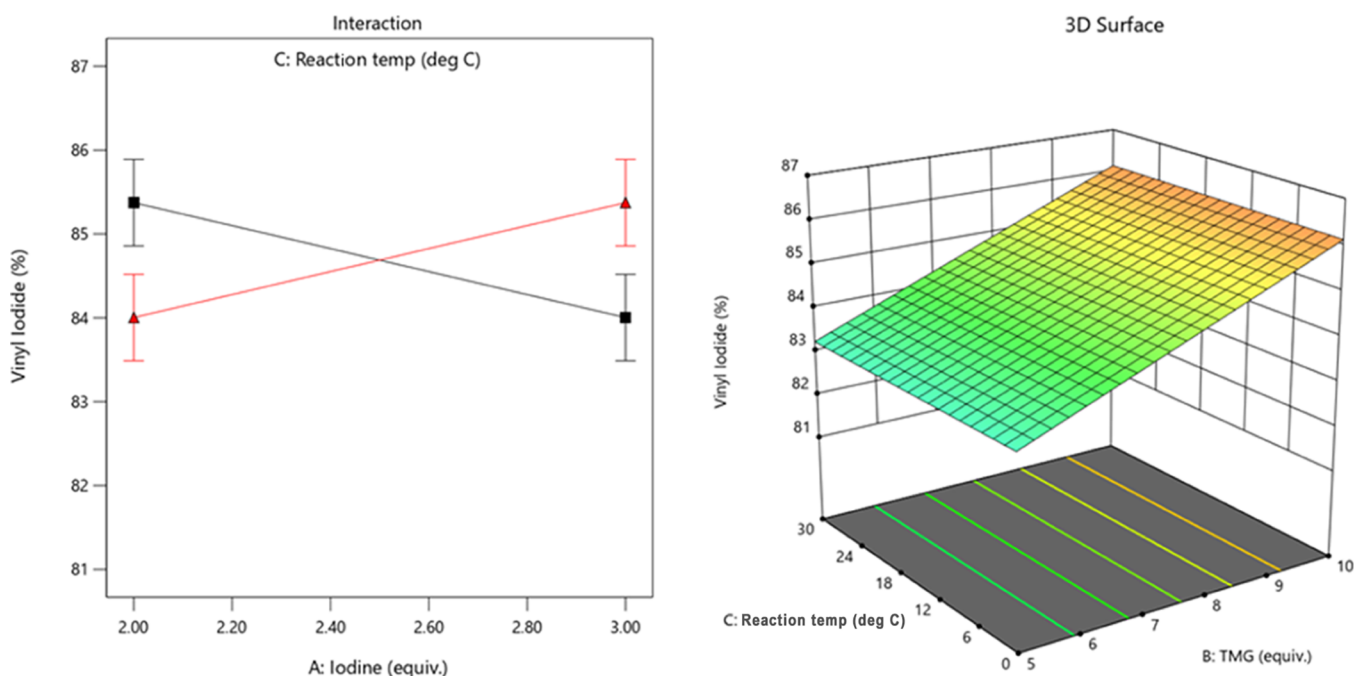
b. Interaction Plot and Contour Plot

Figure 10. Graphical representation of vinyl iodide intermediate **2**.

manually calculated and cross-verified with the PMI calculator.[10,11] The details of the PMI evaluation are listed in Figure 21. This process is favored over the initial process by having about 308 kg less input materials to produce 1 kg of API (further details can be found in the Supporting Information). Process improvements are shown in Scheme 5.

■ CONCLUSIONS

We developed an efficient commercial process for the synthesis of abiraterone acetate by adopting statistical multivariate experimentation. Critical factors in each chemical conversion were identified using fishbone analysis. We were able to establish the relationship between the factors and responses and the

## a. Pareto Chart and Contour Graph
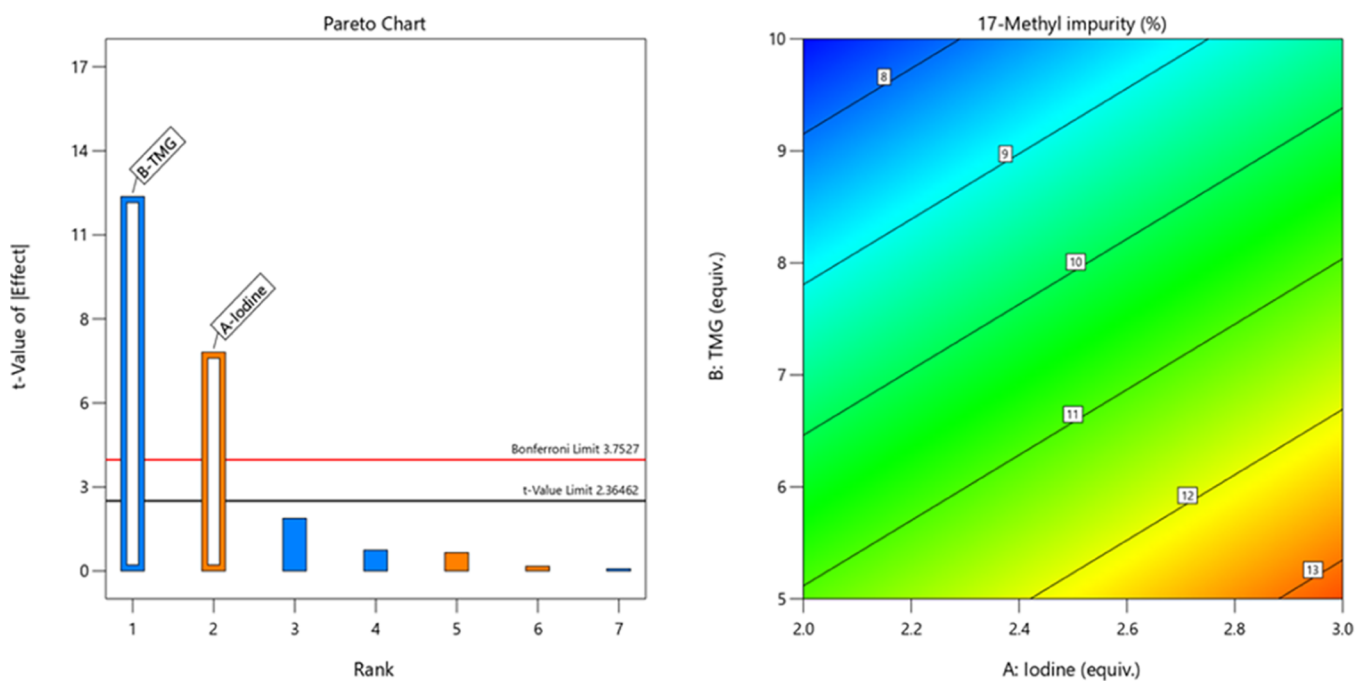
b. Main Effects Graph
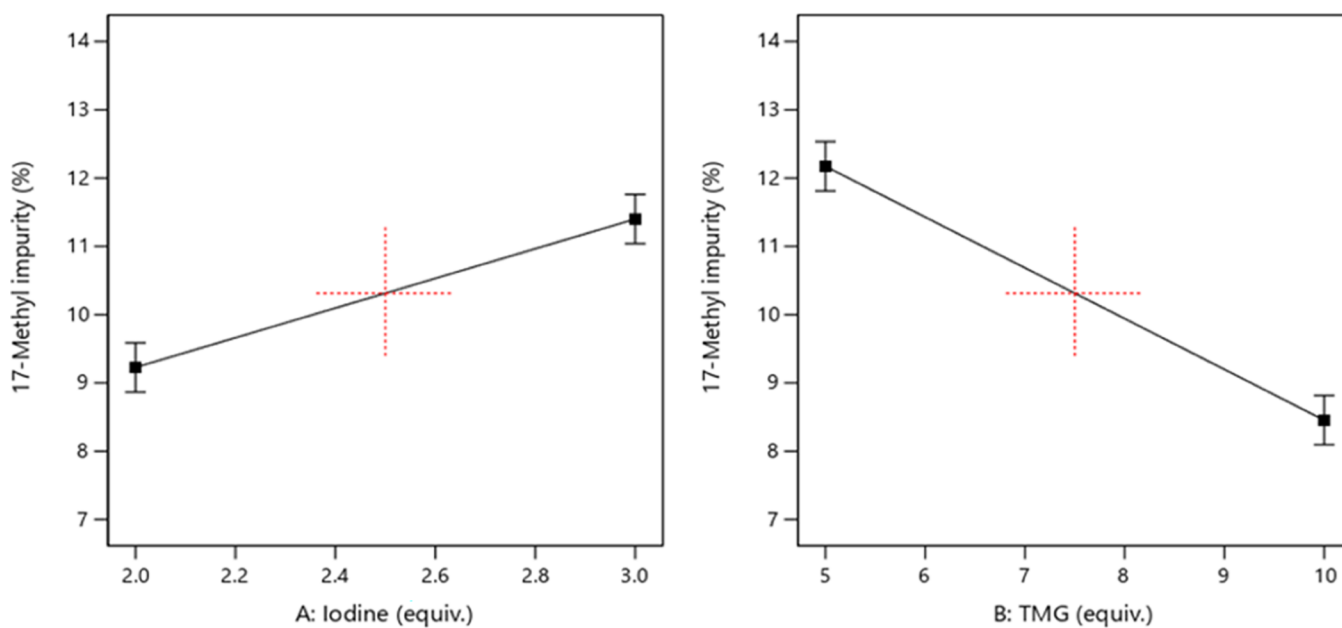
Figure 11. Graphical representation of 17-methyl impurity **6**.

derived design space to define the operating ranges. We have been successful in controlling the formation of potential impurities in each stage so that isolated yields improved to 95% in hydrazone intermediate **3** synthesis, 80% in vinyl iodide intermediate **2**, and 75% in final API **1**. The overall yield jacked up to 57% from 25%; thus, the process efficiency improved.

■ EXPERIMENTAL SECTION

The syntheses of all intermediates and final API were carried out at the Research and Development Center, IPDO, Dr. Reddy's Laboratories Ltd., Telangana., India. All experiments were performed under an inert atmosphere (nitrogen or argon) using commercially available or laboratory reagent-grade chemicals and solvents and maintained anhydrous conditions. Reactions were carried out in a round-bottom flask or cylindrical vessel

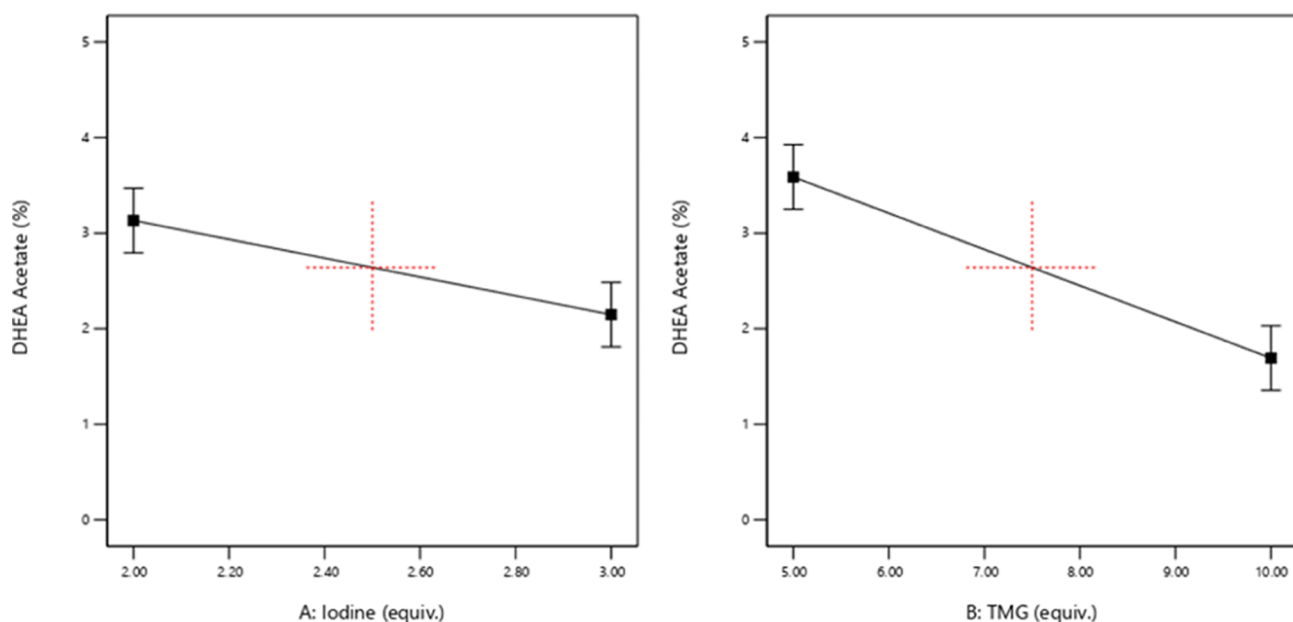# a. Pareto Chart and 3D Graph
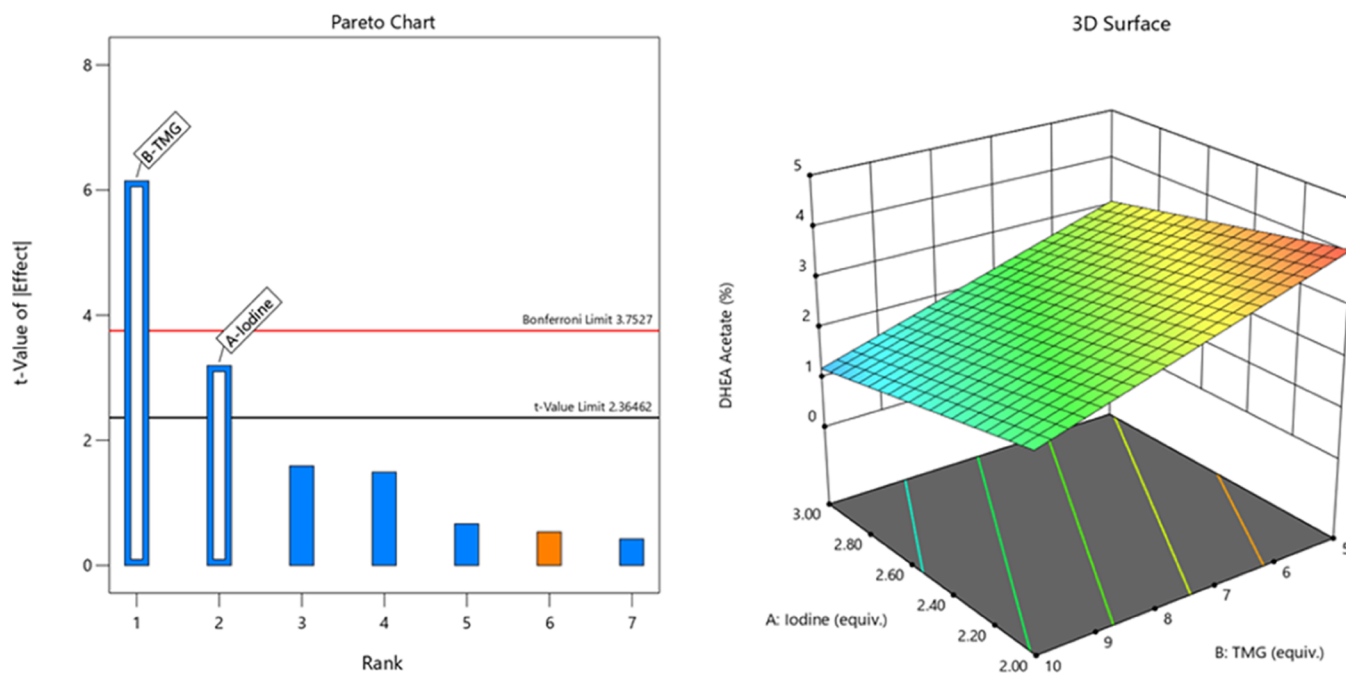
b. Main Effects Graph

Figure 12. Graphical representation of DHEA acetate **4**.

with a mechanical stirrer. Purified water used in the workup process was collected from a Millipore Water purified system. Distillation operations were carried out in a Buchi rotary evaporator system under vacuum, Filtration operations were performed in a Buchner funnel and dried under vacuum in a calibrated vacuum tray dryer. Yields calculated based on the

input and output weights for every intermediate and final product were calculated on dry weight. All materials were stored with proper labels with suitable storage conditions. HPLC-grade acetonitrile and methanol, orthophosphoric acid, potassium dihydrogen phosphate, tetrabutylammonium hydrogen sulfate, and trifluoroacetic acid were procured from Merck Life Science
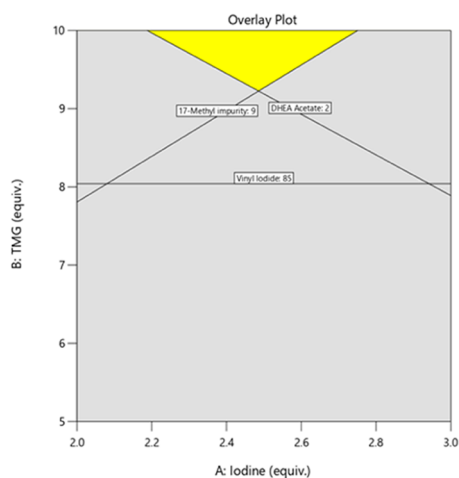
Figure 13. Design space of vinyl iodide intermediate **2** synthesis (15 °C temperature).

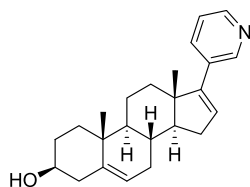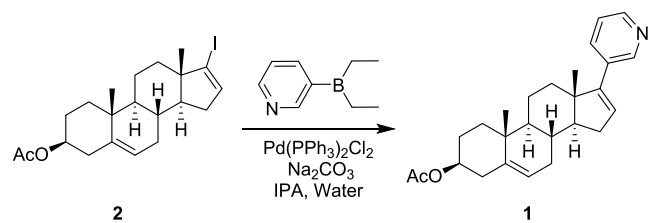**Scheme 4. Synthetic Scheme of Abiraterone Acetate 1**

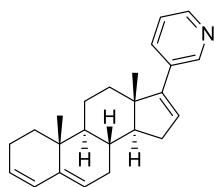**Figure 14.** Chemical structure of hydroxy impurity **8**.

Figure 15. Chemical structure of diene impurity **9**

Pvt. Ltd. (Mumbai, India). Commercial grade reagents, aqueous hydrochloric acid (HCl) from Spectrochem Pvt. Ltd. (Hyder-

Table 5. Factors Studied for the Suzuki Coupling Reaction

s.no.	variables	unit	low	high
1	IPA	vol	2	6
2	BET	equiv	0.95	1.20
3	Na_2CO_3	equiv	4	10

Table 6. Experimental Data of the Suzuki Coupling Reaction

run	IPA vol	BET equiv	Na_2CO_3 equiv	product **1** %	hydroxy impurity **8** %	diene impurity **9** %
1	4	1.08	7	83.47	1.70	1.00
2	6	1.20	4	84.42	0.51	0.77
3	6	0.95	4	83.08	0.40	0.57
4	6	0.95	10	87.43	4.80	0.69
5	6	1.20	10	79.35	5.10	1.68
6	2	0.95	10	84.12	1.50	2.03
7	2	0.95	4	84.19	1.15	1.02
8	4	1.08	7	84.40	1.60	1.10
9	2	1.20	10	82.49	3.20	1.67
10	2	1.20	4	82.66	3.01	1.27

abad, India), 30% hydrogen peroxide (H_2O_2) and sodium hydroxide (NaOH) from Sigma-Aldrich (Hyderabad, India), and Milli-Q purified water by the Milli-Q plus purification system from Millipore (Bradford, PA) were utilized in the course of analysis. NMR solvent $CDCl_3$ was purchased from Cambridge Isotope Laboratories Inc., MA.

^1H and ^{13}C NMR experiments for intermediates, impurities, and API were recorded on a Bruker Avance 400 MHz NMR spectrometer in $CDCl_3$ solvent. The instrument was equipped with a cryogenic probe to regulate the sample temperature at 25 °C. ^1H and ^{13}C chemical shift values were reported with reference to the $CDCl_3$ solvent peak at 7.25 ppm. Mass spectra were recorded using electrospray (ESI) techniques. Low- and high-resolution mass spectra were measured with Finnigan TSQ70 and VG Analytical ZAB2-E instruments, respectively. The FT-IR spectra were recorded on the PerkinElmer model spectrum series FT-IR as a KBR pellet.

A high-performance liquid chromatography instrument was equipped with an ultraviolet spectrophotometer as a detector and an autosampler, a Waters Alliance system, and a data handling system (Waters Millennium32 or Empower pro or equivalent chromatographic software). 1.0 g of potassium dihydrogen phosphate was dissolved in 1000 mL of Milli-Q water. The pH was adjusted to 3.1 ± 0.05 with orthophosphoric acid. The solution was filtered and degassed. 1.0 mL of orthophosphoric acid (85 or 88%) was diluted to 10 mL and
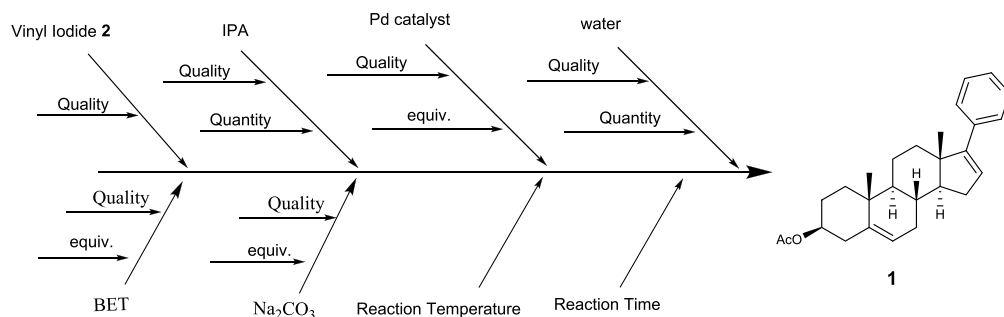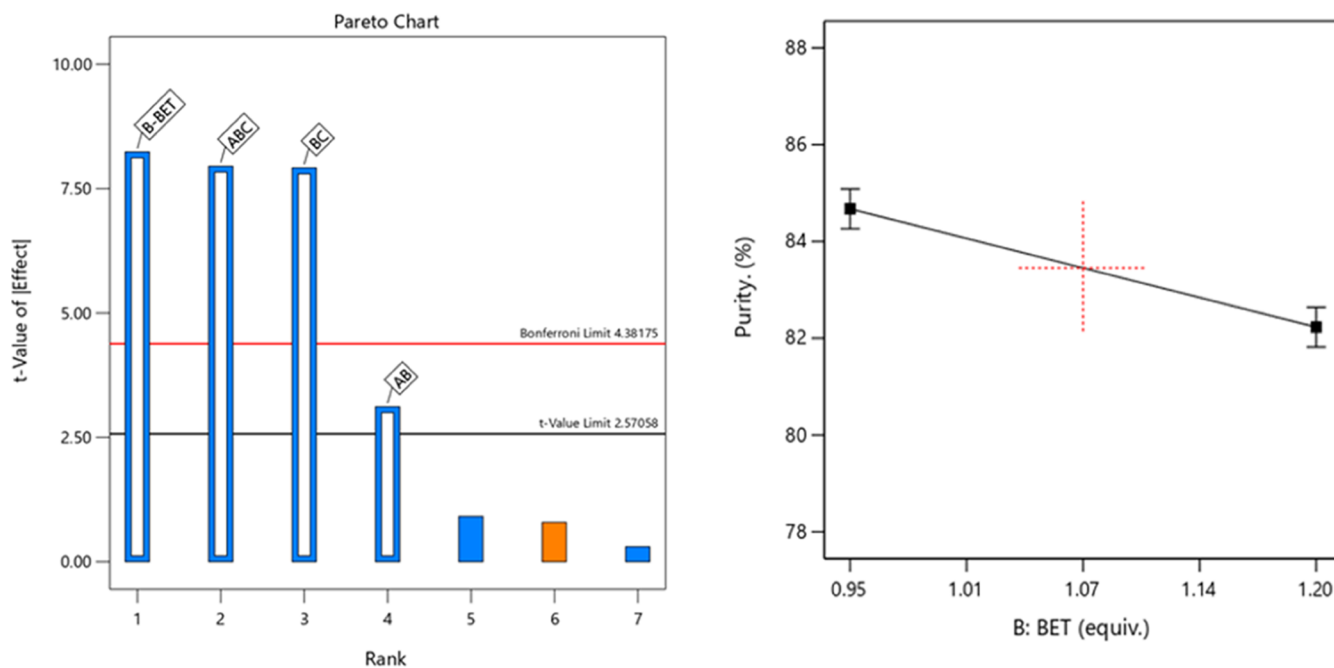

Figure 16. Cause and effect analysis for abiraterone acetate **1** synthesis.

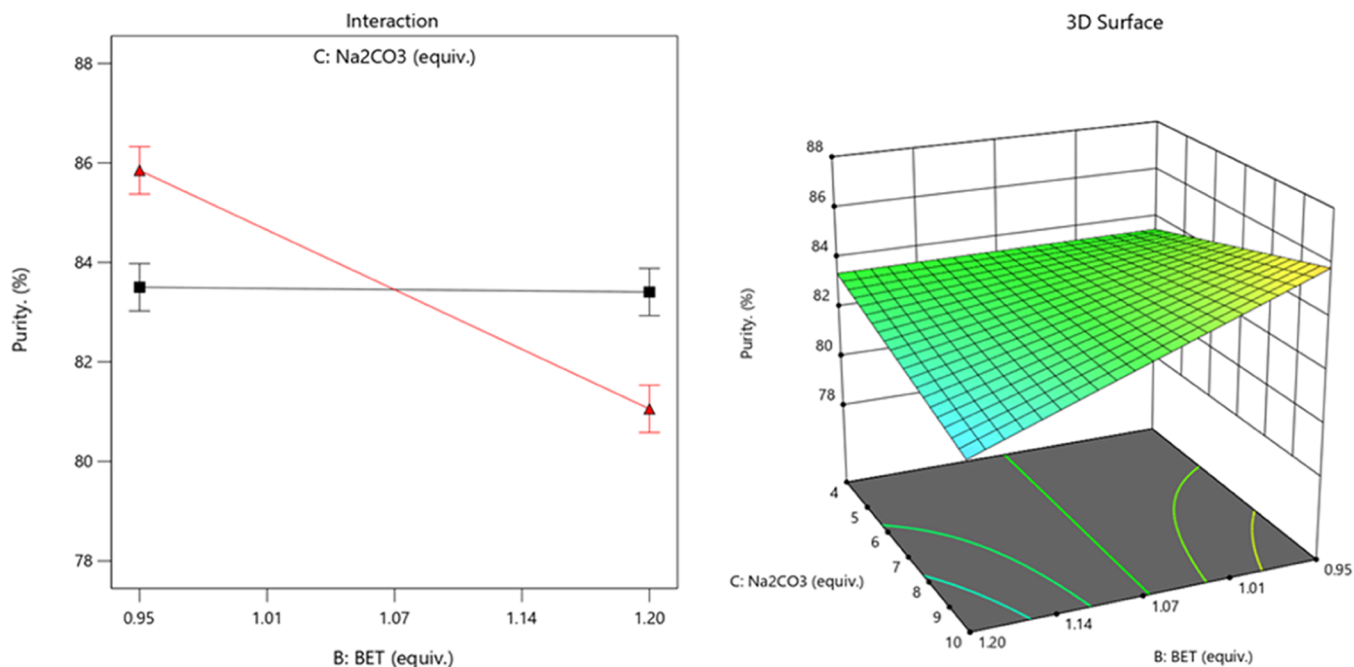# a. Pareto Chart and Main Effects Graph
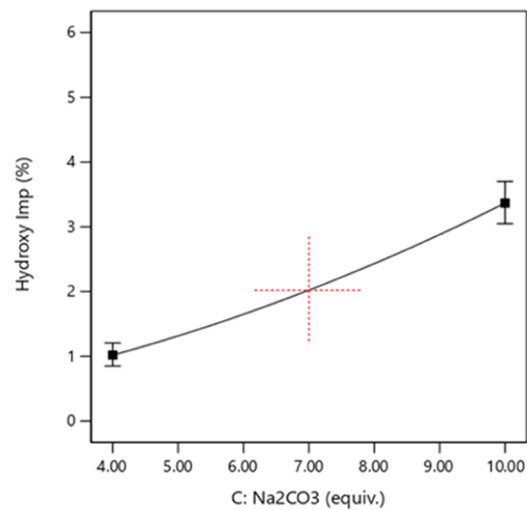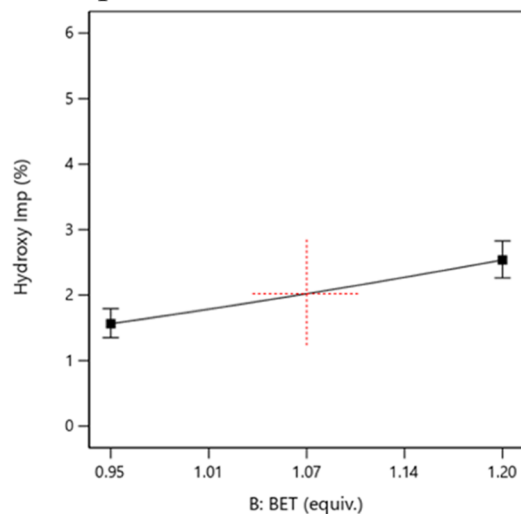

b. Interaction Graph and Contour 3D Graph

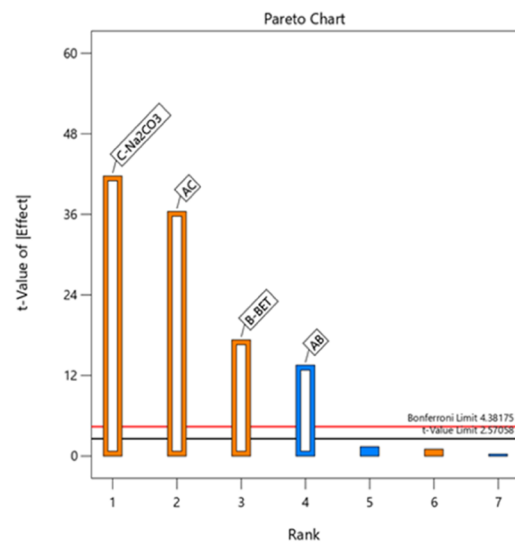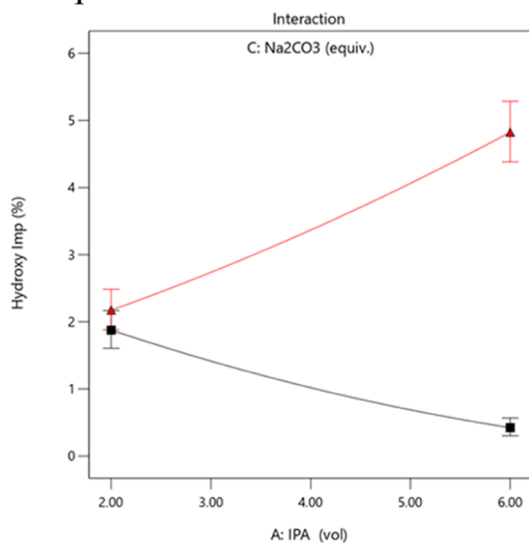**Figure 17.** Graphical representation of product **1**.

used for pH adjustment with a calibrated pH meter. 50 mL of water was pipetted out and added to 950 mL of acetonitrile. The solution was filtered and degassed. Column: Kinetex 5 μm C18 150 mm × 4.6 mm, column temperature: 40 °C, wavelength: 205 nm by UV, injection volume: 10 μL, sample concentration:

2 mg/mL, diluent: acetonitrile/water (70:30), and elution gradient method. The linear gradient program by changing the percentage of mobile phases was as follows: time in min/% mobile phase-A/%mobile phase-B/%mobile phase-C: 0.01/50/

a. Main Effects Graph

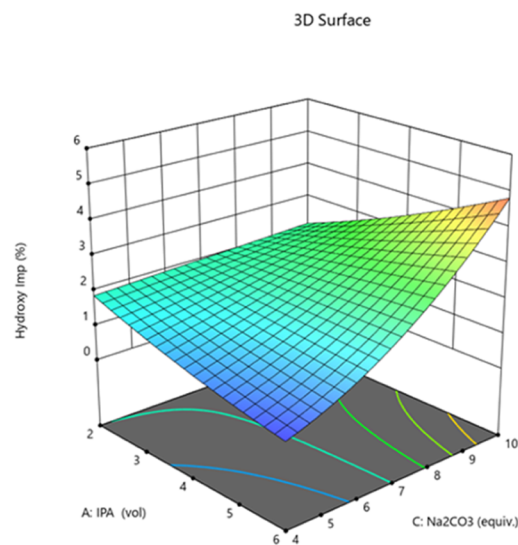**b**. Interaction Graph and Pareto Chart
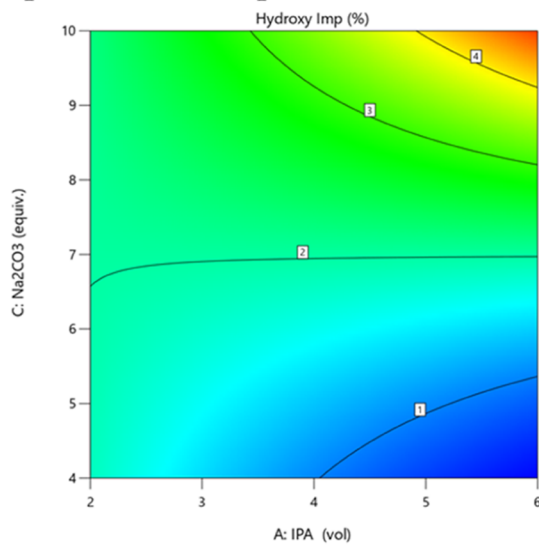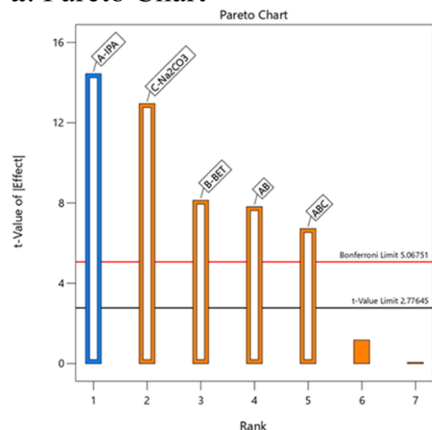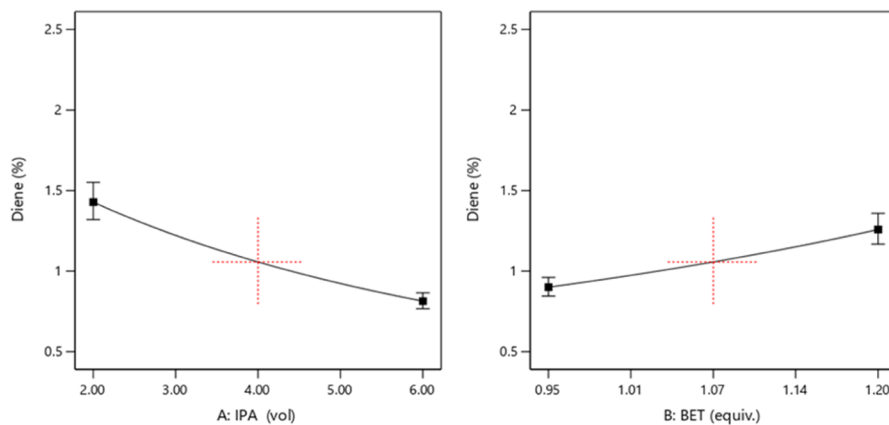

c. Contour Graph and 3D Graph

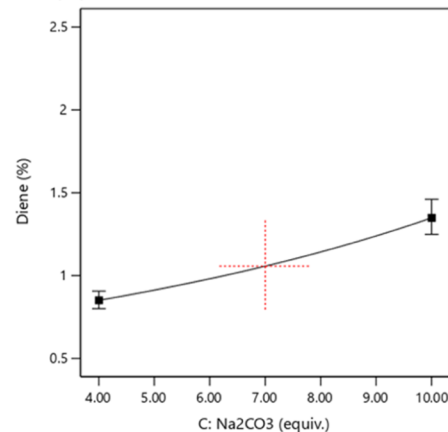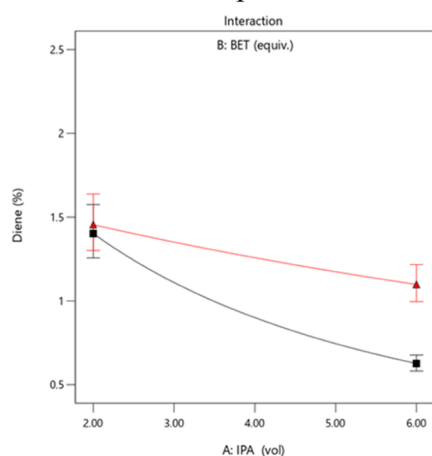**Figure 18.** Graphical representation of hydroxy impurity **8**.
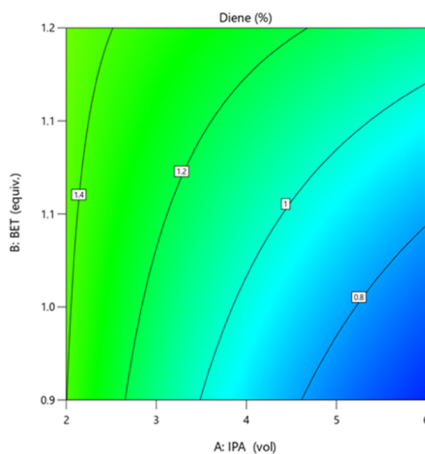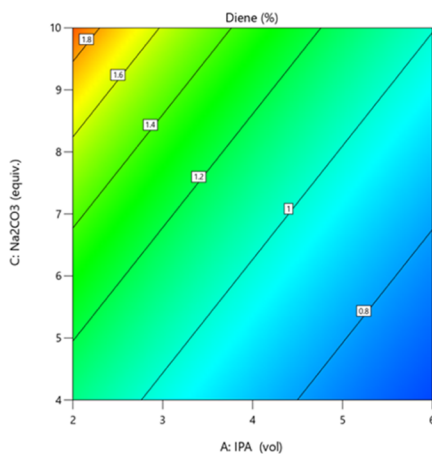
a. Pareto Chart

b. Main Effects Graph

c. Interaction Graph

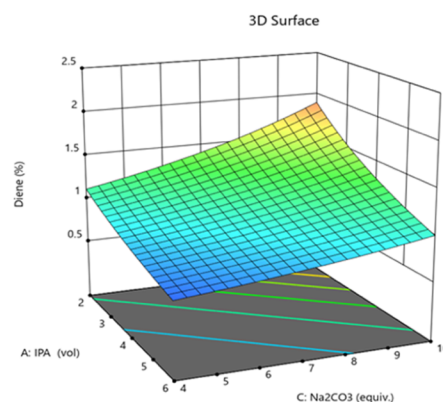**d**. Contour and 3D Graph

e. Contour and 3D Graph

Figure 19. Graphical representation of Diene impurity **9**.

20/30, 40/15/55/30,47/0/20/80, 58/0/20/80, 60/50/20/30, and 70/50/20/30.

Step 1. Hydrazone 3 Synthesis. (3)-Acetoxy-dehydroe-piandrosterone **4** (5 kg, 15.13 mol), ethyl acetate (15 vol, 75 L), and isopropyl alcohol (1 vol, 5 L) were charged into a dry round-bottom flask at 25−30 °C and the mixture was stirred for 5−10 min. Hydrazine hydrate (2.94 L, 58 mol.) was charged, and the reaction mixture was heated to a temperature range of 65−70 °C and stirred at the same temperature for 6 h. The reaction mixture was allowed to cool to 25−35 °C, diluted with ethyl acetate (40

L), and washed with water (2×10 L) and then with an aqueous saturated sodium chloride solution (2×10 L). The organic layer was separated, concentrated under vacuum up to 2 vol, isolated with *n*-heptane wet cake, and dried under vacuum at 40 °C to give hydrazone derivative **3** with 95% yield and 99% purity by HPLC. ^{1}H NMR (400 MHz, Bruker 400 MHz Spectrometer, CDCl$_3$): δ 5.41(d, 1H), 4.6(m, 1H), 4.8(broad, 2H), 2.35(m, 2H), 2.23(m, 2H), 2.21(m, 2H), 2.04(s, 3H), 1.68 (m, 2H), 1.62 (m, 2H), 1.57(m, 2H),1.54 (m, 1H), 1.46 (m, 1H), 1.40 (m, 1H), 1.39 (m, 2H), 1.18(m, 2H), 1.14 (s, 3H), 1.03(s,
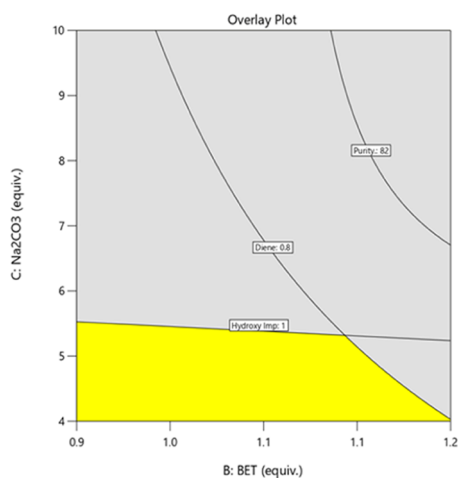
Figure 20. Design space of the Suzuki coupling reaction (5 vol of IPA).

3H).13 C NMR(100 MHz): δ 170.5, 165.8, 139.9, 122.0, 73.8, 53.9, 50.3, 44.0, 38.1, 36.9, 36.7, 34.1, 31.3, 31.2, 27.7, 26.6, 24.3, 23.3, 21.4, 20.6, 19.3. Dip mass analysis of $m/z = 344.49$, found $m/z + 1 = 345$.

Step 2. Vinyl Iodide 2 Synthesis. Iodine (9.21 kg, 36.3 mol) and ethyl acetate (4 vol, 20 L) were charged into a round-bottom flask at 25−30 °C, and the mixture was cooled to 0−5 °C. 1,1,3 3-Tetramethylguanidine (16.73 kg, 145 mol) was charged into an iodine mixture at 0−5 °C. The hydrazone derivative (5 kg, 14.51 mol) was dissolved in ethyl acetate (20 vol, 100 L) and added slowly over a period of 50−60 min. The reaction mixture was stirred at 0−5 °C for 90 min, further heated to 60−65 °C, and stirred for 2−3 h. The reaction mixture was allowed to cool to room temperature, charged water (25 L) was stirred for 1 h, and the organic layer was separated with a 5% sodiumthiosulfate solution (2 vol, 10 L), followed by water and then a 10% sodium chloride solution (2 vol, 10 L). A clear

a. PMI Values Based on Feasibility Process

- Manual calculation based on the feasibility process

  PMI = 493 kg/kg of API

- PMI calculator indicated values

  PMI = 491 kg/kg of API
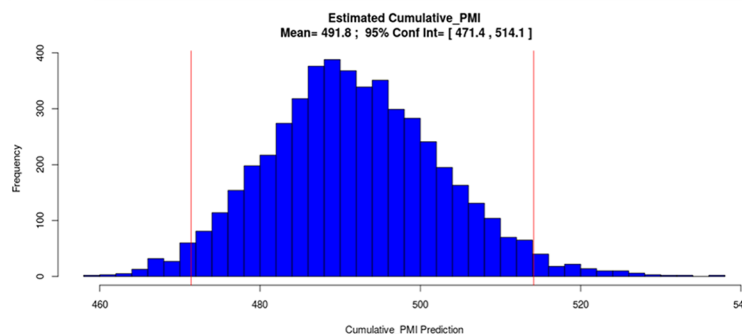
b. PMI Values Based on Optimized Process Disclosed in this Report

- Manual calculation based on the process disclosed in this report

  PMI = 185.2 kg/kg of API

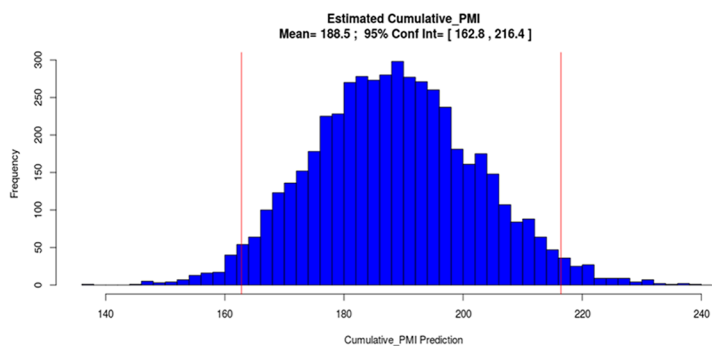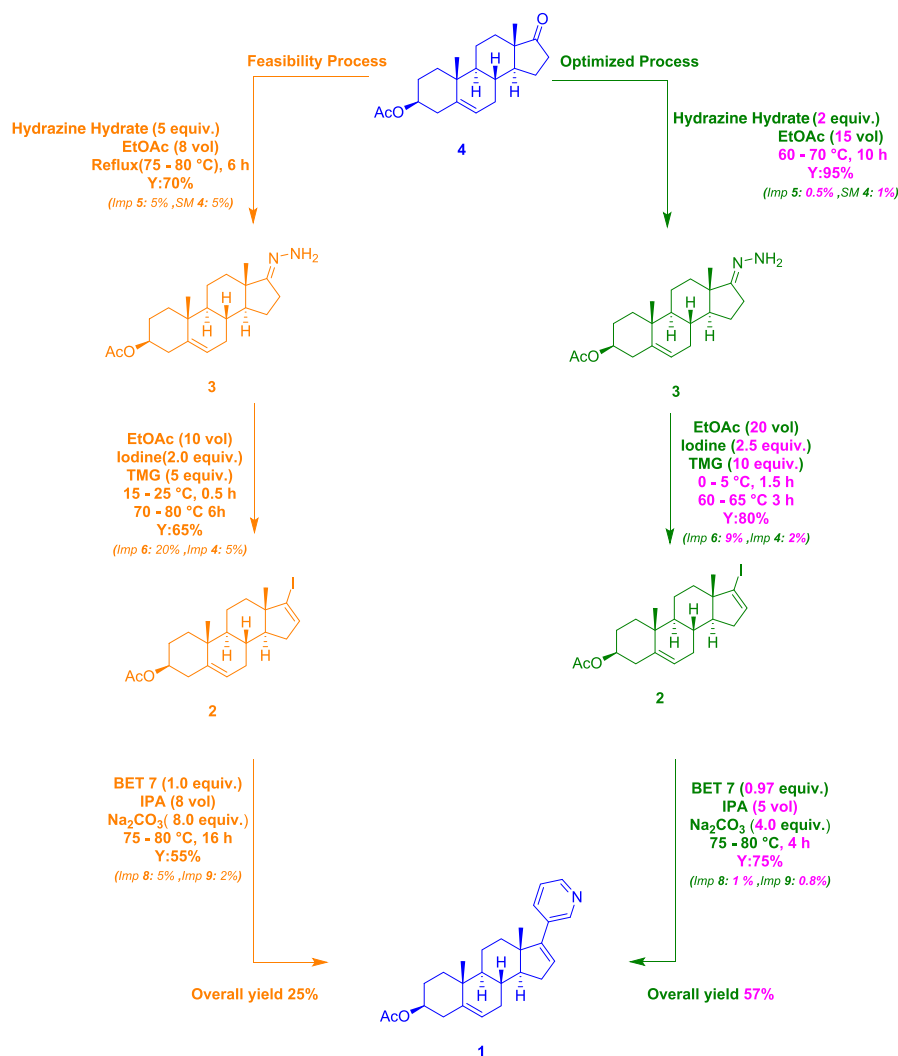- PMI calculator indicated values

  PMI = 188.5 kg/kg of API

Figure 21. PMI comparatives of feasibility (a) and optimization (b).

Scheme 5. Feasibility and Optimization Process Comparison for 1

organic layer was distilled under vacuum up to 3 vol (15 L) and cooled to room temperature. Then, methanol (10 vol, 50 L) was added. The mixture was cooled to 0−5 °C and stirred for 1−2 h. Then, the solid was filtered, and the wet cake was washed with chilled methanol (2 vol, 10 L) and dried under vacuum at 45−50 °C for about 4 h to give vinyl iodide **2**. Yield: 5.43 kg (85%). Purity by HPLC: 96%. ^{1}H NMR (400 MHz, Bruker 400 MHz Spectrometer, CDCl$_3$): δ 6.10 (t, 1H), 5.37(t, 1H), 4.5(m, 1H), 2.37(m, 1H), 2.33(m, 1H), 2.21(s, 3H), 2.12(m, 1H), 2.08(m, 1H), 2.04 (m, 1H), 1.79(m, 1H), 1.78(m, 1H), 1.66(m, 1H), 1.53(m, 1H), 1.52(m, 1H), 1.48(m, 1H), 1.45(m, 1H), 1.44(m, 1H), 1.41(m, 1H), 1.38(m, 1H), 1.27(m, 2H), 1.13(m, 1H), 1.01(s, 3H), 1.01(s, 3H).[13] C NMR(100 MHz): δ 170.5, 140.1, 137.5, 122.1, 112.6, 73.8, 54.7, 50.4, 49.9, 38.1, 36.9, 36.8, 36.1, 33.7, 31.2, 31.0, 27.7, 21.4, 20.7, 19.2, 15.1. Dip mass analysis of m/z = 440.36, found M + NH$_4$ + 1 = 458.2.

Step 3. Suzuki Coupling Reaction. Vinyl iodide **2** ((3S,8R,9S,10R,13S,14S)-17-iodo-10,13-dimethyl-2,3,4,7,8,9,10,11,12,13,14,15-dodecahydro-1H-cyclopenta[a]-phenanthren-3-yl acetate) (5 kg, 11.36 mol), isopropanol (5 vol, 25 L), and water (8 vol, 40 L) were charged into a round-bottom flask at room temperature, and the mixture was stirred for 10 min. Diethyl(3-pyridyl)borane (1.62 kg, 11.0 mol), bis-(triphenylphosphine)palladium(II)dichloride (0.1 kg, 0.136

mol), and sodium carbonate (4.82 kg, 45 mol) were charged in sequence to the reaction mixture and stirred for 10 min. The reaction mixture was heated to a temperature range of 75−80 °C and stirred for about 4−6 h at the same temperature. The reaction mixture was allowed to cool to 25−30 °C, followed by addition of toluene (50 L) and stirring for about 60 min. The two layers were separated, followed by washing the organic layer with a 10% aqueous sodium chloride solution (10 L). Triethylamine (3.18 L, 22.7 mol), dimethyl amino pyridine (13.8 g, 0.1136 mol), acetic anhydride (1.74 L, 17 mol), and the organic layer were put in a round-bottom flask, and the reaction mixture was stirred at 25−30 °C for 90 min; water (20 L) was added to the reaction mass slowly at below 20 °C. The reaction mixture was stirred for 30 min, and the layers were separated. The obtained organic layer was washed with water (20 L), followed by a 10% aqueous sodium chloride solution (20 L). The organic layer was separated and charged acetone (10 L) and oxalic acid (1.71 kg), stirred for 1 h and filtered the solid. Oxalate salt was neutralised using aqueous sodium carbonate solution (15 L). Free base was dissolved in acetone (52 L) at 40 °C. The reaction mixture was cooled to room temperature. Then, water (52 L) was added slowly over 30 min and stirred for 1 h, and the solid obtained was filtered under vacuum, washed with acetone (2 L), and dried under vacuum at 40 °C to give the title

compound. Yield: 2.86 kg (65%); HPLC purity: >99.5%. ^{1}H NMR (400 MHz, Bruker 400 MHz Spectrometer,CDCl$_3$): δ 8.55(s, 1H), 8.39(d, 1H), 7.60(d, 1H), 7.20(m, 1H), 5.96(s, 1H), 5.35(d, 1H), 4.50(m, 1H), 2.12(m, 1H), 2.06(m, 2H), 2.04(m, 2H), 2.02(s, 3H), 1.94(m, 1H), 1.66(m, 2H), 1.52(m, 2H), 1.48(m, 1H), 1.45(m, 1H), 1.41(m, 2H), 1.38(m, 1H), 1.13(m, 1H), 1.10(m, 1H), 1.01(s, 6H). ^{13}C NMR(100 MHz): δ 170.4, 151.6, 147.8, 147.8, 140.0, 133.7, 132.9, 129.2, 123.0, 122.2, 73.8, 57.4, 50.2, 47.3, 38.1, 36.9, 36.7, 35.2, 31.8, 31.5, 30.4, 27.7, 21.4, 20.8, 19.2, 16.5. Dip mass analysis of $m/z = 391$, found $m/z + 1 = 392$.

ASSOCIATED CONTENT

Supporting Information

The Supporting Information is available free of charge at https://pubs.acs.org/doi/10.1021/acsomega.4c01912.

General details; experimental section; instrumental details; statistical analysis containing ANOVA table, fit statistics and graphical representations of every response variable, and spectral data of all compounds; and PMI evolution details (PDF)

AUTHOR INFORMATION

Corresponding Authors

Rakeshwar Bandichhor − *Dr. Reddy's Laboratories Ltd., Integrated Product Development, Innovation Plaza, Bachupally, Hyderabad 500090 Telangana, India;* orcid.org/0000-0003-2673-1429; Phone: +91 9000770751; Email: rakeshwarb@drreddys.com; Fax: +91 40 44346285

Arthanareeswari Maruthapillai − *Department of Chemistry, Faculty of Engineering and Technology, SRM Institute of Science and Technology, Kattankulathur 603203 Tamil Nadu, India;* orcid.org/0000-0003-4246-6856; Phone: +91 44 27417832; Email: arthanam@srmist.edu.in

Authors

Shravan Kumar Komati − *Department of Chemistry, Faculty of Engineering and Technology, SRM Institute of Science and Technology, Kattankulathur 603203 Tamil Nadu, India; Dr. Reddy's Laboratories Ltd., Integrated Product Development, Innovation Plaza, Bachupally, Hyderabad 500090 Telangana, India*

Mukesh Kumar Madhra − *Dr. Reddy's Laboratories Ltd., Integrated Product Development, Innovation Plaza, Bachupally, Hyderabad 500090 Telangana, India*

Amarendhar Manda − *Department of Chemistry, Faculty of Engineering and Technology, SRM Institute of Science and Technology, Kattankulathur 603203 Tamil Nadu, India; Dr. Reddy's Laboratories Ltd., Integrated Product Development, Innovation Plaza, Bachupally, Hyderabad 500090 Telangana, India*

Sasikala Cheemalapati Venkata Annapurna − *Dr. Reddy's Laboratories Ltd., Integrated Product Development, Innovation Plaza, Bachupally, Hyderabad 500090 Telangana, India*

Gopal Chandru Senadi − *Department of Chemistry, Faculty of Engineering and Technology, SRM Institute of Science and Technology, Kattankulathur 603203 Tamil Nadu, India;* orcid.org/0000-0003-0149-5423

Complete contact information is available at: https://pubs.acs.org/10.1021/acsomega.4c01912

Notes

ACKNOWLEDGMENTS

ABBREVIATIONS

QbD quality by design
DHEA dehydroepiandrosterone
BET diethyl(3-pyridyl)borane
API active pharmaceutical ingredient
CQA critical quality attribute
CPP critical process parameter
CMA critical material attribute
HPLC high-performance liquid chromatography
ANOVA analysis of variance
SM starting material
DoE design of experiments
TMG tetramethylguanidine
NMT not more than
IPA isopropyl alcohol

REFERENCES

(1) Thakur, A.; Roya, A.; Ghosh, A.; Chhabra, M.; Banerjee, S. Abiraterone acetate in the treatment of prostate cancer. *Biomed. Pharmacother.* **2018**, *101*, 211−218.

(2) Balaev, A. N.; Gromyko, A. V.; Fedorov, V. E. Four-Step Synthesis of Abiraterone Acetate from Dehydroepiandrosterone. *Pharm. Chem. J.* **2016**, *50*, 404−406.

(3) Barton, D. H. R.; Pradhan, S. K.; Sternhell, S.; Templeton, J. F. Triterpenoids. Part XXV. The constitutions of limonin and related bitter principles. *J. Chem. Soc.* **1961**, 255−275.

(4) Kubota, T.; Matsuura, T.; Tokoroyama, T.; Kamikawa, T.; Matsumoto, T. Establishment of the correlation of obacunone and limonin. *Tetrahedron Lett.* **1961**, *2*, 325−332.

(5) Barton, D. H. R.; O'Brien, R. E.; Sternhell, S. A new reaction of hydrazones. *J. Chem. Soc.* **1962**, 470−476.

(6) Barton, D. H. R.; Bashiardes, G.; Fourrey, J. L. An improved preparation of vinyl iodides. *Tetrahedron Lett.* **1983**, *24*, 1605−1608.

(7) Barton, D. H. R.; Bashiardes, G.; Fourrey, J. L. Studies on the oxidation of hydrazones with iodine and with phenylselenenyl bromide in the presence of strong organic bases; an improved procedure for the synthesis of vinyl iodides and phenyl-vinyl selenides. *Tetrahedron Lett.* **1988**, *44*, 147−162.

(8) Potter, G. A.; Hardcastle, I. R.; Jarman, M. A Convenient, large-scale synthesis of Abiraterone acetate [3β-Acetoxy-17-(3-Pyridyl) Androsta-5, 16-Dien, Potential New Drug for the treatment of prostate cancer. *Org. Prep. Proced. Int.* **1997**, *29*, 123−128.

(9) Liu, Y.; Liu, L.; Shi, G.; Shi, J.; Lai, W. L. Research on the synthesis and characterization of abiraterone acetate. *Bulg. Chem. Commun.* **2017**, *49*, 199−203.

(10) Hochberg, R. B.; McDonald, P. D.; Ponticorvo, L.; Lieberman, S. Identification of 17-methyl-18-norandrosta-5, 13 (17-dien-3beta-ol, the C19 fragment formed by adrenal side chain cleavage of a 20-aryl analog of (20S)-20-hydroxycholesterol. *J. Biol. Chem.* **1976**, *251*, 7336−7342.

(11) PMI Calculator. https://acsgcipr-predictpmi.shinyapps.io/pmi_calculator/.

(12) Žigart, N.; Časar, Z. Development of a stability-indicating analytical method for determination of venetoclax using AQbD principles. *ACS Omega* **2020**, *5*, 17726−17742.

(13) Metil, D. S.; Sonawane, S. P.; Pachore, S. S.; Mohammad, A.; Dahanukar, V. H.; McCormack, P. J.; Bandichhor, R. Synthesis and optimization of canagliflozin by employing quality by design (QbD) principles. *Org. Process Res. Dev.* **2018**, *22*, 27−39.

(14) Montgomery, D. C. *Design and Analysis of Experiments*; John wiley & sons, 2017.

(15) Foschi, M.; Capasso, P.; Maggi, M. A.; Ruggieri, F.; Fioravanti, G. Experimental Design and Response Surface Methodology Applied to Graphene Oxide Reduction for Adsorption of Triazine Herbicides. *ACS Omega* **2021**, *6*, 16943−16954.

(16) Wang, H.; Chen, K.; Lin, B.; Kou, J.; Li, L.; Wu, S.; Liao, S.; Sun, G.; Pu, J.; Yang, H.; Wang, Z. Process Development and Optimization of Linagliptin Aided by the Design of Experiments (DoE). *Org. Process Res. Dev.* **2022**, *26*, 3254−3264.

(17) Department of Health and Human Services, U.S. Food and Drug Administration. In *ICH Q8 Pharmaceutical Development (R2)*; Center for Drug Evaluation and Research (CDER): Rockville, MD, 2009.

(18) Department of Health and Human Services, U.S. Food and Drug Administration. In *ICH Q9 Quality Risk Management*; Center for Drug Evaluation and Research (CDER): Rockville, MD, 2009.

(19) Department of Health and Human Services, U.S. Food and Drug Administration. In *ICH Q10 Pharmaceutical Quality System*; Center for Drug Evaluation and Research (CDER): Rockville, MD, 2009.

(20) Abe, Y.; Emori, K. Application of a Statistical Approach to Process Development of Futibatinib by Employing Quality-by-Design Principles. Part 2: Development of Design Space for Impurities Using the Response Surface Methodology. *Org. Process Res. Dev.* **2022**, *26*, 56−71.